Journal of Power Sources 203 (2012) 34–41

Contents lists available at SciVerse ScienceDirect

Journal of Power Sources

journal homepage: www.elsevier.com/locate/jpowsour

Electrochemical characteristics of nano-structured $PrBaCo_2O_{5+x}$ cathodes fabricated with ion impregnation process

Yao Wang[a], Han Zhang[a], Fanglin Chen[a,b], Changrong Xia[a,*]

[a] CAS Key Laboratory of Materials for Energy Conversion, Department of Materials Science and Engineering, University of Science and Technology of China, Hefei, Anhui 230026, China
[b] Department of Mechanical Engineering, University of South Carolina, Columbia, SC 29208, USA

ARTICLE INFO

Article history:
Received 30 September 2011
Received in revised form
23 November 2011
Accepted 24 November 2011
Available online 3 December 2011

Keywords:
Praseodymium barium cobalt oxide
Impregnation
Layered-structure cobaltite
Cathode
Solid oxide fuel cells

ABSTRACT

Nano-structured electro-catalyst of layered-structure cobaltite $PrBaCo_2O_{5+x}$ (PBC) has been developed as cathode for solid oxide fuel cells (SOFCs) and excellent electrochemical activity towards oxygen reduction has been achieved. PBC nano-particles are deposited into porous samaria-doped ceria (SDC) backbones with an impregnation method. The fabrication processing parameters including composition of precursor solution, PBC loading, and firing temperature have been investigated to optimize the cathode microstructure and further to minimize the cathode interfacial polarization resistance, leading to a cathode interfacial polarization resistance of only $0.082\,\Omega\,cm^2$ at 600 °C, much lower than those reported for pure PBC electrode ($0.86\,\Omega\,cm^2$), PBC–SDC composite cathode ($0.25\,\Omega\,cm^2$) or various other impregnated cobaltite cathodes such as $Sm_{0.5}Sr_{0.5}CoO_{3-\delta}$ ($0.25\,\Omega\,cm^2$), $La_{0.5}Sr_{0.5}CoO_{3-\delta}$ ($0.31\,\Omega\,cm^2$), and $La_{0.6}Sr_{0.4}Co_{0.2}Fe_{0.8}O_{3-\delta}$ ($0.24\,\Omega\,cm^2$). The novel nano-structured PBC electrochemical reaction mechanism has found to be similar to that of a conventional PBC cathode. However, both oxygen ion incorporation and charge transfer steps are greatly accelerated for the novel nano-structured PBC cathode, suggesting that the impregnation process is very effective in fabricating layered-structure cobaltite electro-catalyst for intermediate-temperature SOFC cathode with enhanced electrode performance.

1. Introduction

Solid oxide fuel cell (SOFC) cathodes are usually composites consisting of ABO_3 perovskites such as $(La_{0.85}Sr_{0.15})_{0.9}MnO_{3-\delta}$ (LSM) [1], $La_{0.5}Sr_{0.5}CoO_{3-\delta}$ (LSC) [2], $La_{0.6}Sr_{0.4}Co_{0.2}Fe_{0.8}O_{3-\delta}$ (LSCF) [3] and $Ba_{0.5}Sr_{0.5}Co_{0.8}Fe_{0.2}O_{3-\delta}$ (BSCF) [4]. Recently, layered cobaltites such as $PrBaCo_2O_{5+x}$ (PBC) and $GaBaCo_2O_{5+x}$ (GBC) have also been studied as potential SOFC cathode. In the layered structure, Ba-cations reside in alternating (0 0 1) layers while oxygen vacancies are located in the rare earth planes [5]. This particular distribution of vacancies could greatly enhance the diffusivity of oxide ions in the bulk of the material and possibly supply surface defect sites with enhanced reactivity towards oxygen reduction compared with non-ordered ABO_3 perovskites. For example, the oxygen surface exchange coefficient of PBC at 350 °C is about $10^{-3}\,cm\,s^{-1}$ [6], much higher than that of BSCF ($2\times10^{-5}\,cm\,s^{-1}$ at 600 °C) [7], LSC ($2\times10^{-6}\,cm\,s^{-1}$ at 600 °C) [8], and LSCF ($1\times10^{-4}\,cm\,s^{-1}$ at 800 °C) [9]. Preliminary studies by Chang et al. [10] have shown that the interfacial polarization resistance of GBC electrodes on $Ce_{0.8}Gd_{0.2}O_{1.96}$ electrolytes is as low as $0.53\,\Omega\,cm^2$ at 645 °C. Much higher electrode performance has been reported by Shao et al. [11] with PBC as the SOFC cathode. The resistance is only $0.40\,\Omega\,cm^2$ at 600 °C when samarium-doped ceria (SDC) is used as the electrolyte. This is probably due to the much higher oxygen ion diffusion coefficient of PBC compared with that of GBC [6]. The chemical compatibility [12] of the layered cobaltites with typical electrolytes such as $Zr_{0.84}Y_{0.16}O_{1.92}$ (YSZ), $La_{0.8}Sr_{0.2}Ga_{0.8}Mg_{0.2}O_{3-\delta}$ (LSGM) and $Ce_{0.9}Gd_{0.1}O_{1.95}$ (GDC) has been also evaluated: PBC reacts with YSZ at temperatures as low as 700 °C but is chemically compatible with GDC and LSGM up to 1000 °C. These results have demonstrated that PBC could be a promising cathode material for intermediate-temperature SOFCs.

The electrode performance may be further improved using impregnation method, which is performed by precipitation and subsequent decomposition of a metal salt into porous pre-formed backbones [13–15]. The impregnated electrodes have quite different microstructures from the composite electrodes fabricated with conventional ceramic processing technique. It usually consists of fine particles and porous backbones, which are the same materials as the electrolytes for ion-conducting. This structure has high stability since the backbone and the electrolyte layer are co-fired. Further, the impregnated particles can be high-performed metallic or oxide electro-catalysts such as LSM and LSC. The desired phases are conducted at temperature much lower than that needed

* Corresponding author. Tel.: +86 551 3607475; fax: +86 551 3601592.
E-mail address: xiacr@ustc.edu.cn (C. Xia).

0378-7753/$ – see front matter © 2011 Elsevier B.V. All rights reserved.
doi:10.1016/j.jpowsour.2011.11.069

Table 1
Chemicals of the precursor solutions.

	Chemicals of the precursor solution
PBC1	$Pr(AC)_3 + Ba(AC)_2 + Co(AC)_2$
PBC2	$Pr(AC)_3 + Ba(AC)_2 + Co(AC)_2$ + glycine
PBC3	$Pr(NO_3)_3 + Ba(NO_3)_2 + Co(NO_3)_2$ + citric acid

for the traditional ceramic fabrication process, resulting in nano-sized particles, which are benefit to achieve larger TPB length. This novel cathode microstructure also exhibits high electrochemical performance due to high catalytic activities of nano-structured electro-catalysts with large specific area, and high oxygen ion transport rate through the well structured backbones with extended three phase boundaries [13–17]. For example, LSC impregnated electrode [18] has exhibited interfacial polarization resistance as low as 0.30 $\Omega\,cm^2$ at 600 °C. With LSM impregnated cathodes, single cells have exhibited peak power density of 780 $mW\,cm^{-2}$ at 700 °C [19].

In this work, PBC is used as the electro-catalyst, which has been impregnated onto porous SDC backbones. The fabrication conditions are optimized regarding composition of the precursor solution, PBC loading, and firing temperature. The reaction mechanism of the impregnated PBC electrodes has been evaluated by analysis of the oxygen partial pressure dependence of the polarization resistance and active energy in each sub-step. Performance of single cells with such cathodes has also been investigated.

2. Experimental

SDC ($Sm_{0.2}Ce_{0.8}O_{1.9}$) powder was prepared using glycine–nitrate process, which was described as follows: stoichiometric amounts of the nitrate precursors $Ce(NO_3)_3$ and $Sm(NO_3)_3$ with the nominal composition were dissolved in distilled water. Glycine was then added to the solution at a mole ratio of 1:2 for glycine:nitrate ions. The precursor solution was subsequently heated on a hot plate till self-combustion occurred. The resulting ashes were calcined at 600 °C for 2 h to remove possible organic residues and to form the desired fluorite structure of doped ceria. NiO powder was also prepared with the glycine–nitrate process and formed by firing the ashes at 850 °C for 4 h.

Symmetrical cells were composed of SDC electrolyte substrates, porous SDC backbones co-fired with the substrates, and $PrBaCo_2O_{5+x}$ (PBC) electro-catalysts impregnated into the backbones. The SDC powders were cold-pressed at 250 MPa to form green substrates with diameter of 15 mm. SDC slurry prepared by mixing SDC powders with an organic binder (α-terpineol as the solvent and ethyl cellulose as the binder) was then printed onto both sides of the substrates. After drying under an infrared lamp, the sandwich fresh bodies were co-fired at 1400 °C for 5 h to form symmetrical cell structures [18], i.e. porous SDC backbones supported on both sides of the dense SDC electrolytes.

Three different impregnation solutions (as shown in Table 1) were prepared with the metal ion concentration of 0.1 M. Ion impregnation was carried out by placing a drop of the solution on the top of the SDC frame, letting the solution soak into the porous backbones, drying, and firing the sample at 800 °C in air for 1 h to form PBC particles. The mass of the sample before and after each impregnation treatment was measured to estimate the impregnated material loading, which was expressed as the mass ratio of the impregnated oxides to the backbones.

Single cells had a configuration of Ni-SDC anode substrates, SDC film electrolytes, and impregnated cathodes. The anode powders consisting of 60 wt.% NiO and SDC were mixed and pressed at 30 MPa. SDC powder as the electrolyte was subsequently added on the top of the pre-pressed pellet and co-pressed at 180 MPa to form a green bi-layer structure: a thin SDC layer supported on a thick NiO-SDC layer [18]. SDC slurry was then printed on top of the electrolyte followed by drying under an infrared lamp to form a tri-layer structure, which was subsequently co-sintered at 1250 °C for 5 h to densify the electrolyte layer. PBC was then impregnated on the porous SDC backbone to form a single cell consisting of Ni-SDC composite substrate (the anode), a dense SDC electrolyte, and PBC impregnated SDC frame (the cathode). PBC2 was used as the precursor solution for the single cell preparation.

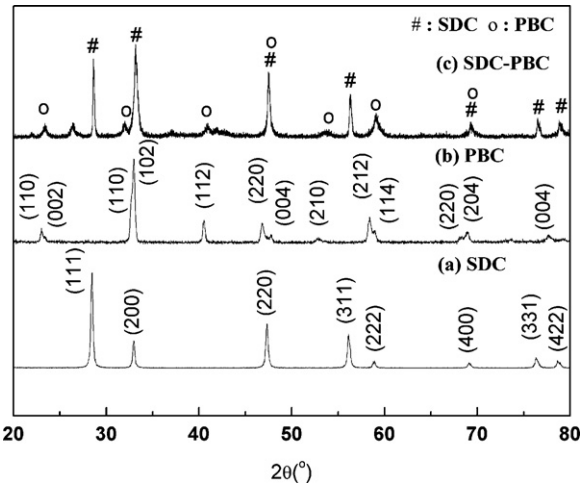

Fig. 1. XRD patterns of (a) SDC powder fired at 800 °C for 2 h, (b) PBC powder fired at 800 °C for 2 h, and (c) porous SDC backbones impregnated with PBC solution and fired at 800 °C for 1 h.

The phase structure was characterized by X-ray diffraction (Rigaku TTR-III). The morphology of the cell was observed using a scanning electron microscope (SEM, FEI XL30). EIS measurements were carried out with a Zahner Im6ex electrochemical workstation under open circuit conditions at oxygen partial pressures from 0.01 atm to 1 atm formed by mixing O_2 with N_2 using mass flow controllers. The frequency ranged from 10^{-1}–10^{-2} to 10^6 Hz with amplitude of 10 mV. AC impedance plots were fitted using Zview software according to proper equivalent circuit with a standard deviation below 5%. The performance of the single cell was evaluated using humidified (~3% H_2O) hydrogen as the fuel with a flow rate of 100 ml min^{-1} and ambient air as the oxidant.

3. Results and discussion

3.1. Structures of the impregnated phase

Fig. 1 shows the XRD pattern of an impregnated structure, along with the XRD patterns of SDC and PBC powders for comparison. The results demonstrate that the impregnated sample is composed of the orthorhombic phase of PBC and the cubic phase of SDC without any other phases, suggesting that there is no obvious chemical reaction between SDC and PBC under the experimental conditions and that the impregnated substance forms orthorhombic PBC when it is fired at 800 °C for 1 h. The crystallite size of the PBC particles is calculated to be 20 nm according to the Scherrer equation performed on the (1 1 2) diffraction. Previous work has shown that PBC is compatible with SDC up to 1000 °C [12]. This work demonstrates that the impregnated substance does not react with SDC and can form PBC phase at 800 °C in the presence of SDC. Further, it has been found that lowing the firing temperature <800 °C cannot form the desired PBC phase while increasing the firing temperature above 800 °C results in coarsening of the PBC particles.

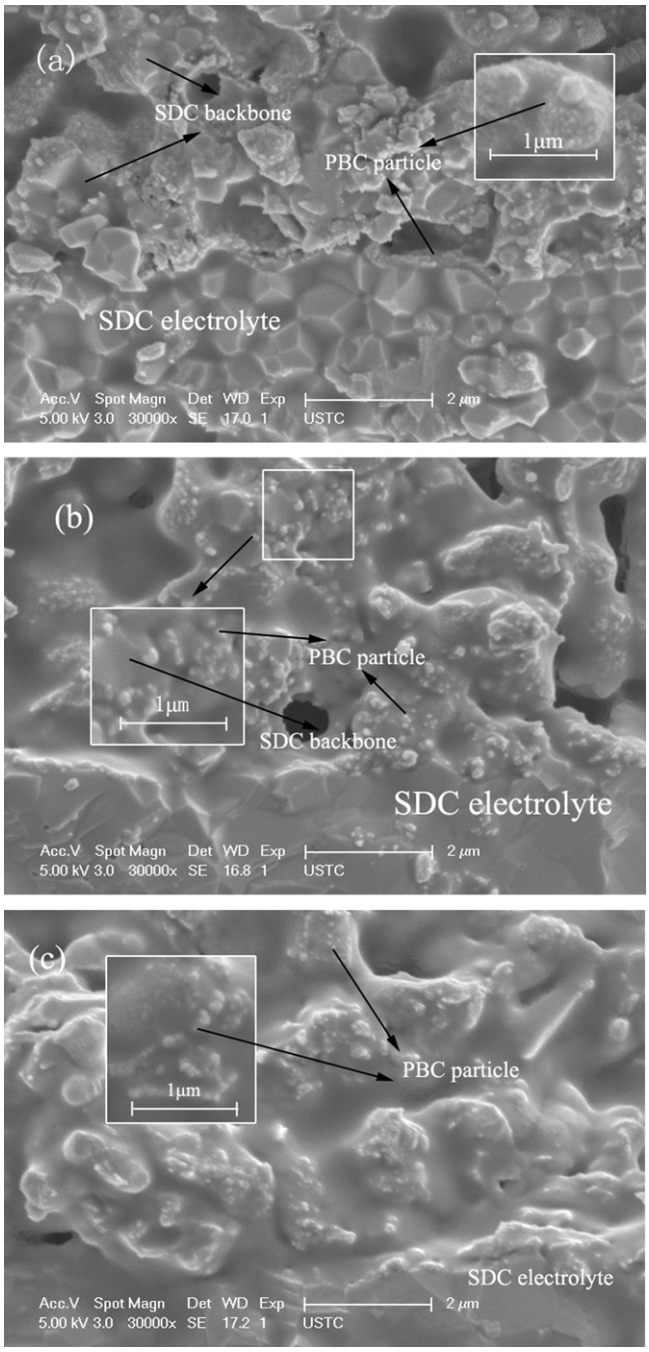

Fig. 2. Cross-sectional SEM graphs for the microview of the electrode/electrolyte where PBC are impregnated with different precursor solution. (a) acetate, PBC1, (b) acetate with glycine, PBC2, and (c) nitrate with citric acid, PBC3. The loading is about 30%.

The impregnation precursors are critical in preparing nanostructured electro-catalysts since they determine the microstructures and even the composition of the infiltrated particles [14,20,21]. Fig. 2a shows the cross-sectional view of the electrode/electrolyte interface where PBC particles are synthesized from acetate, PBC1. The PBC particles are very fine and seem to form a uniform continuous layer on the inner surface of the porous SDC backbone down to the electrolyte/backbone interface. When glycine is added, as shown in Fig. 2b, the distribution of the impregnated particles becomes more uniform. The particles are still very fine. The size is about 50 nm but increases slightly compared with that shown in Fig. 2a. Glycine acts as not only a chelating agent but also a burning-assisted chemical. Gas released in the combustion process blocks the secondary aggregation, while high heat flow could cause grain growth. Fig. 2b also shows that the impregnated particles seem to be anchored into the backbones, and the adhesion between the electrolyte and electrode is greatly enhanced. The unique microstructure may be beneficial to the oxygen reduction process. When the PBC particles are prepared from nitrates with citric acid, PBC3, as shown in Fig. 2c, a different microstructure is observed with irregular growth of PBC particles, possibly due to the high heat flow caused by the combustion process with citric acid, which releases more heat than that with glycine.

3.2. Effects of PBC loading

In addition to the composition of the precursors, the microstructures as well as the electrode performance are greatly affected by the loading of the infiltrated particles. When the loading is very low, infiltrated particles cannot form a continuous network, and the electrochemical performance is limited. If the loaded mass is too much, charge/gas transport can be inhibited because of the aggregation of impregnated particles, and the performance is also restricted. Consequently, there exists an optimized loading for the infiltrated electrodes, which has also been demonstrated by modeling analysis [22]. Fig. 3a shows the total interfacial polarization resistance measured at 600, 650, and 700 °C for cathodes impregnated with 16.37%, 21.25%, 30.63% and 39.82% PBC1. The resistance at 600 °C decreases from 0.485 Ω cm^2 to the lowest of 0.160 Ω cm^2 when the loading increases from 16.37% to 30.63%. Further increasing the loading to 39.82% results in slight increase in resistance, 0.162 Ω cm^2. Therefore, Fig. 3a shows that the optimized loading for PBC1 infiltrated electrode is about 30%. Similar loading effect on the interfacial resistance has also been observed for the other two impregnation compositions (Fig. 3b and c). The lowest resistance is achieved at the loading of 29.4% for PBC2 and 33.1% for PBC3. Although the precursor solutions are different, these electrodes exhibit the best performance at roughly the same loading, about 30%. Fig. 3d shows the comparison of the Arrhenius plots for the cathodes with the optimized electro-catalyst loading. The resistances and activation energies are different for the different impregnation compositions, indicating that the starting precursor solutions have great effects on the electrode performance in addition to the electrode microstructures. The electrode derived with PBC2 exhibits the smallest dependence on temperature with an activation energy of 0.95 eV, much lower than 1.03 eV for PBC1 and 1.60 eV for PBC3. Moreover, this electrode shows the highest performance, especially in lower temperature range. For instance, the resistance at 600 °C is 0.082 Ω cm^2, only about half of 0.160 Ω cm^2 for PBC1 and 0.174 Ω cm^2 for PBC3. This result is consistent with that from the SEM observation. In addition, the obtained cathode interfacial resistance of 0.082 Ω cm^2 is much lower than 0.31 Ω cm^2 for impregnated LSC [18], 0.24 Ω cm^2 for impregnated LSCF [3], 0.25 Ω cm^2 for impregnated SSC [23], and 1.82 Ω cm^2 for impregnated LSM [24]. Therefore, the impregnated PBC electrode has shown the highest performance among the impregnated electrodes prepared under similar conditions, as shown in Fig. 4.

3.3. Cathode reaction mechanism

It is generally accepted that the reaction for a composite cathode with the normal random distributed structure may be controlled by gas diffusion, surface adsorption, dissociation, electron and ion charge transfer and so on. To distinguish the individual step of the PBC impregnated SDC electrode, impedance spectra of SDC-PBC2/SDC/SDC-PBC2 symmetrical cells are measured at temperature between 500 and 650 °C with oxygen partial pressure from 0.01 to 1 atm. The experimental data in Nyquist plots and the

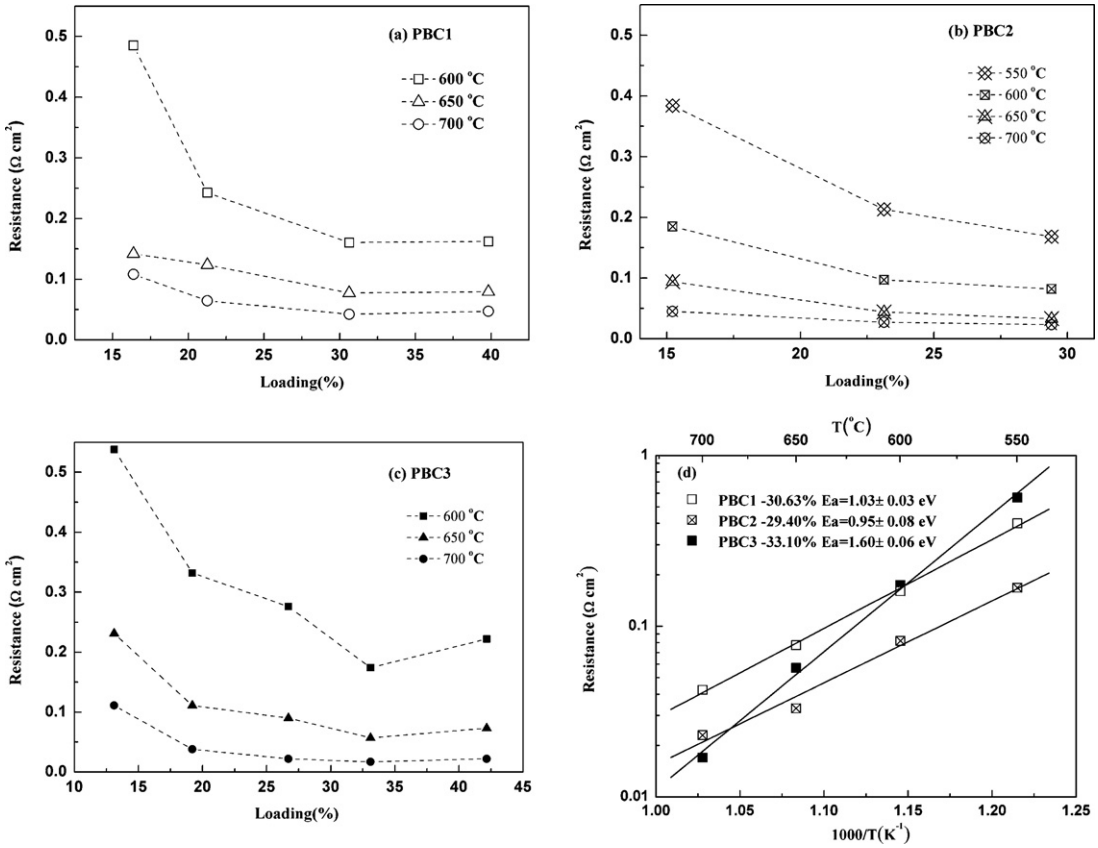

Fig. 3. Effect of loading on the interfacial polarization resistance for electrodes impregnated with different precursor solutions. (a) acetate, PBC1, (b) acetate with glycine, PBC2, (c) nitrate with citric acid, PBC3, and (d) Arrhenius plots for their optimized loadings.

fitting results are present in Fig. 5. The impedance spectra show good agreement with the equivalent circuit $LR_b(RiCPEi)$. Here L is the inductance arising from the apparatus, R_b is attributed to the resistance of the electrolyte, and $(RiCPEi)$ describes a sub-step in the cathode reaction process identified by the range of its frequency, which appears as a depressed semi-circle in Nyquist plots. As it can be seen in Fig. 5, R_b, the first intercept on the real axis has been simplified to zero for better comparison of the electrode resistance. The high frequency arc (R_1CPE_1) could only be observed at 500 and 550 °C and disappears when the temperature is above 600 °C. The middle frequency arc is considered as double equivalent circuit

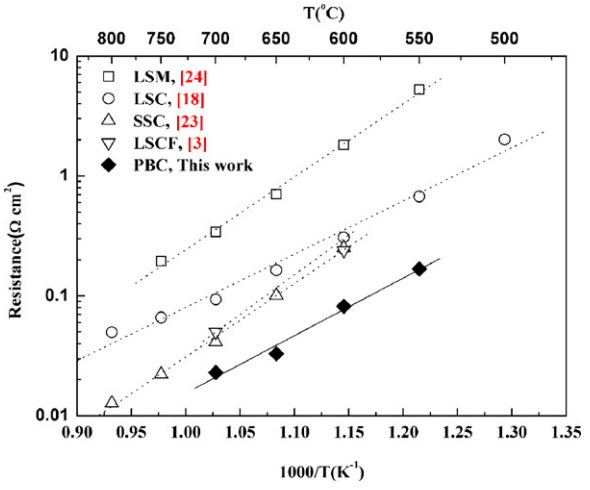

Fig. 4. Interfacial polarization resistance for various impregnated electrodes with SDC backbones.

elements (R_2CPE_2) and (R_3CPE_3), which are not easily distinguishable as they have similar relaxation time constants. An additional depressed arc (R_4CPE_4) at low frequency is also observed at low oxygen partial pressure and high temperature.

The parameter m is commonly used to identify the sub-step of cathode reaction, which normally indicates the relationship between the resistance and oxygen partial pressure, P_{O_2} [25]. The relationship is $R_i = kP_{O_2}^{-m}$, where k is a constant. Fig. 6a shows the value of m for R_1 at high frequency is almost 0, suggesting that R_1 is independent on P_{O_2}. This behavior agrees well with the characteristics of the oxygen ion incorporation from the three phase boundaries (TPB) to the electrolyte, $O^{2-}_{TPB} + V^{\bullet\bullet}_{O,electrolyte} \rightarrow O^{\times}_{O,electrolyte}$ [25,26], a step closely related to the adhesion of the electrolyte/electrode and TPB length. R_1 is about 0.16 Ω cm² at 500 °C in air, and only 10% of that for a pure PBC cathode with the conventional microstructure [11]. The substantial decrease in R_1 is attributed to the unique backbone structure of the impregnated electrode, and also to the enhanced bonding between the very fine embedded PBC particles and the SDC electrolyte as revealed in Fig. 2b. Another evidence for the enhanced oxygen ion incorporation rate can also be obtained from the equivalent capacitance of (R_1CPE_1), which corresponds to the TPB length. Larger capacitance means larger TPB length, and thus more transfer paths for oxygen ion incorporation. The value of the equivalent capacitance for (R_1CPE_1) at 500 °C is about 0.67 μF cm⁻² for pure PBC [11]. However, it is 18.4 μF cm⁻² when only 15.2% PBC2 is impregnated, possibly due to the highly dispersed nano-sized PBC particles which have a larger specific area that can accelerate the process of oxygen ion incorporation.

The angular relaxation frequencies of (R_2CPE_2) and (R_3CPE_3) are in range of 10^3–1 Hz, the typical range for electron charge transfer

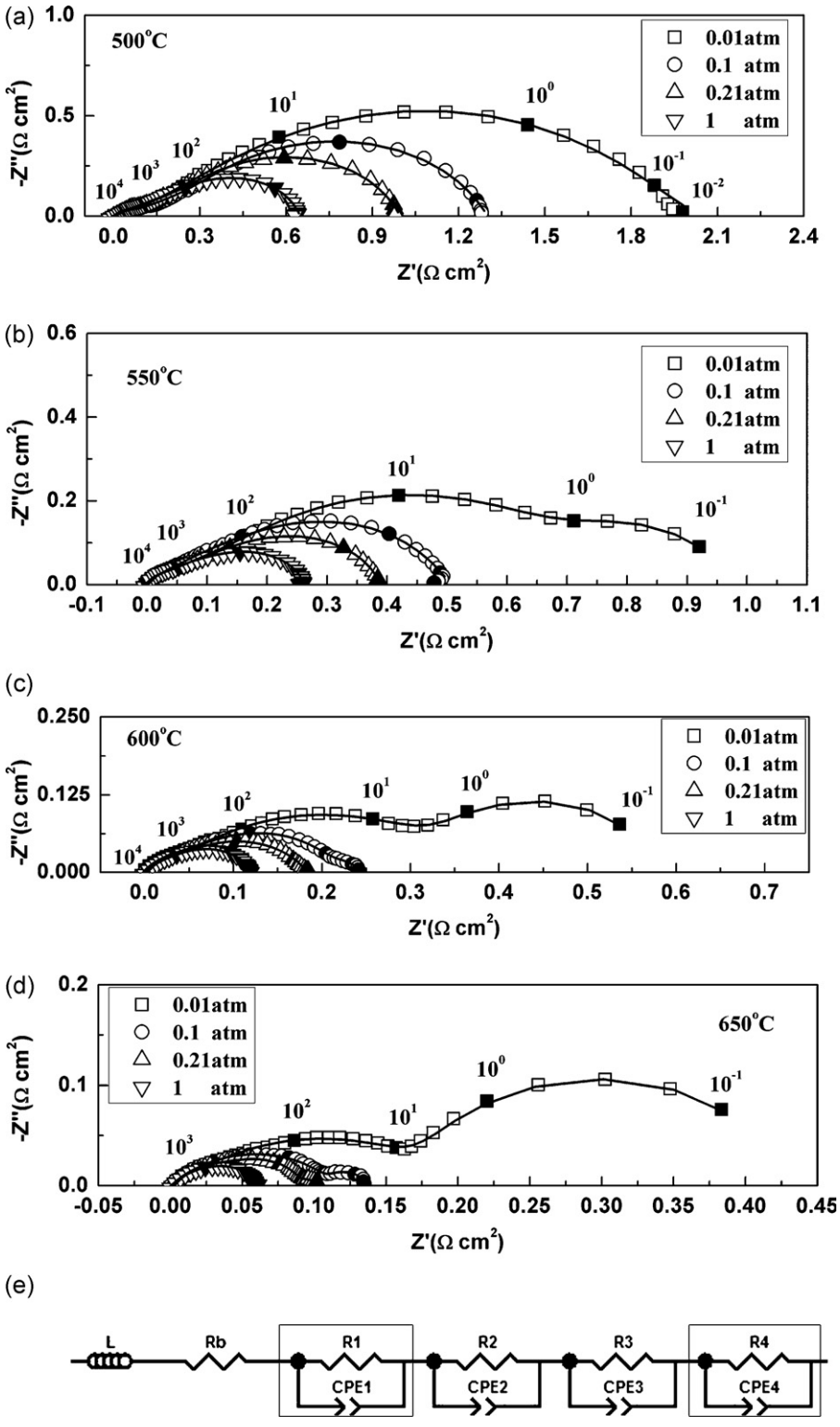

Fig. 5. Impedance spectra for symmetrical cells with the electrode prepared from PBC2 solution under the open-circuit condition. The loading is 15.21%. (a) 500 °C, (b) 550 °C, (c) 600 °C, (d) 650 °C, and (f) equivalent circuit used for fitting the impedance spectra. Symbols and solid lines represent the experimental data and fitted line.

process, $O_{ad} + 2e' + V_O^{\bullet\bullet} \rightarrow O_O^{\times}$, which has a dependence on oxygen partial pressure with $m = 0.25$ [27]. As shown in Fig. 6b and c, m for R_2 is in the range of 0.21–0.23 and R_3 is 0.24–0.28, both are close to the characteristic parameter of 0.25. Therefore, the medium frequency process is attributed to the electron charge transfer. The activation energies (E_a) of R_2 and R_3 are independent on the oxygen partial pressure. As shown in Fig. 7, E_a for R_2 ranges from 0.90 to 0.97 eV, while R_3 varies from 0.82 to 0.95 eV. The activation energies are much lower than those for common cathodes which can be as high as 1.39 eV [28]. The electron charge transfer resistance at 600 °C is 0.195 Ω cm^2, less than 50% of the pure PBC electrode [11]. It can be also attributed to the fine particles of

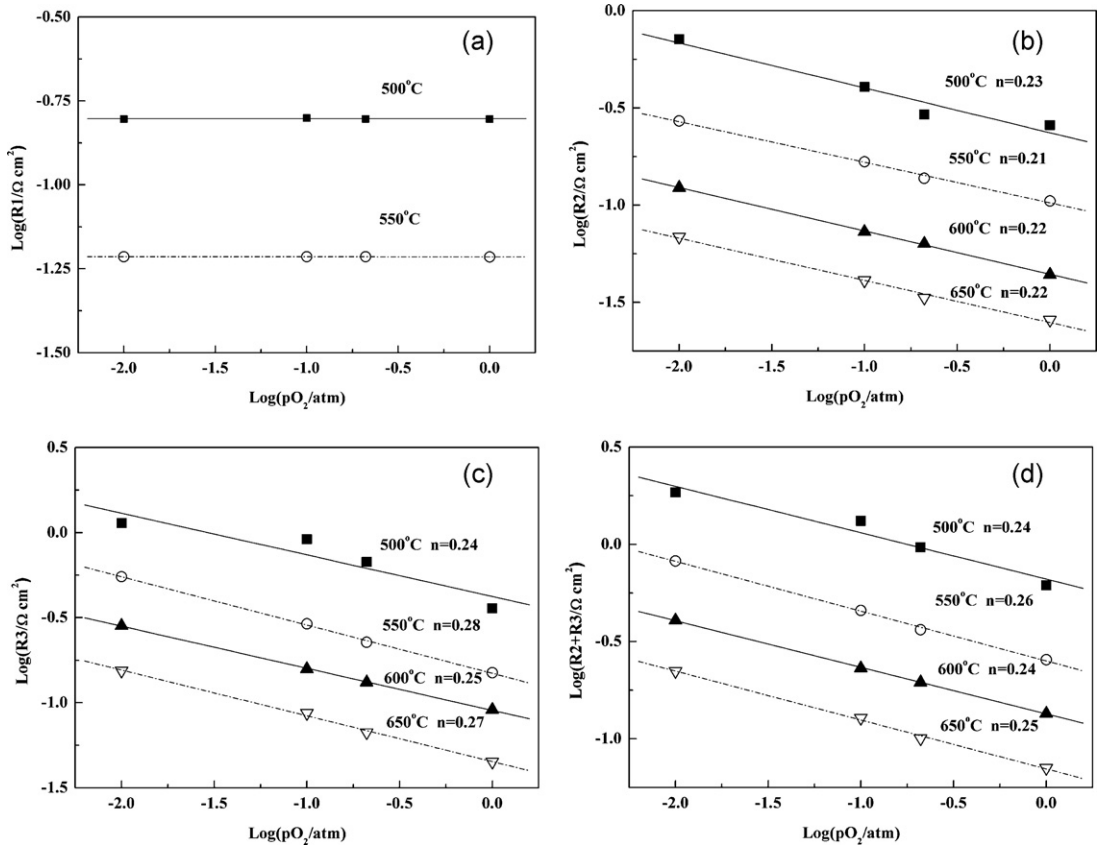

Fig. 6. Dependence of the resistance for the high and medium frequency arcs on oxygen partial pressure. (a) R_1, (b) R_2, (c) R_3, and (d) $R_2 + R_3$.

the impregnated PBC. It is further reduced to 0.082 Ω cm^2 when 29.4% PBC is impregnated, demonstrating significant advantages of the impregnated electrodes.

The low frequency arc is strongly affected by the oxygen partial pressure. The arc could not be observed at $P_{O_2} = 1$ atm in the whole range of temperatures tested, while it becomes dominant at $P_{O_2} = 0.01$ atm, especially at high temperatures. For example, at 650 °C, R_4 is only 0.028 Ω cm^2 at 0.1 atm, but rapidly increases to 0.250 Ω cm^2 at 0.01 atm. The reaction order m is calculated to be 0.95, close to 1, characteristic of the diffusion of oxygen molecules in the electrode pores. The activation energy calculated from the temperature dependence of R_4 is about 0.18 eV, close to 0.14 eV for the oxygen diffusion [24]. Therefore, the low-frequency arc is possibly attributed to the gas phase diffusion step.

Based on the above analysis, for the impregnated PBC cathode, the high frequency arc corresponds to oxygen ion incorporation, the media arcs to charge transfer, and the low arc to gas diffusion. This is almost the same as that derived from pure PBC cathode with the conventional microstructure. However, these processes are significantly accelerated with the impregnated structure. The reaction mechanism is quite different from that for conventional SDC–PBC composite electrodes, where the charge transfer step dominates at high frequencies and surface diffusion prevails at low frequencies [29]. The total interfacial polarization resistance for the 15.2% impregnated PBC2 electrode at 600 °C is 0.195 Ω cm^2, much lower than 0.86 Ω cm^2 for pure PBC and 0.25 Ω cm^2 for the SDC–PBC (30 wt.%) composite electrodes. Moreover, when about 30% PBC is loaded, the resistance is only 0.082 Ω cm^2, significantly lower than that of the SDC–PBC composite electrode. Therefore, impregnation can substantially enhance the electrochemical performance while does not change the cathode reaction process.

3.4. Single cell performance

Performance of the impregnated PBC cathode is further investigated using single cells with Ni-SDC anodes and 26 μm-thick SDC electrolytes. Humidified H_2 (~3% H_2O) is supplied as the fuel and ambient air as the oxidant. Fig. 8 shows the cell voltage and power density as a function of different current densities and cell operating temperatures. A peak power density of 600 mW cm^{-2} has been achieved at 600 °C and the cell performance is comparable to those reported for highly performed single cells with even thinner electrolytes (Table 2). AC impedance spectra under open-circuit conditions are shown in Fig. 9. The total cell resistance at 600 °C is

Table 2
Peak power density (P), ohmic resistance (R_o), and interfacial polarization resistance (R_p) at 600 °C for various single cells with Co-based cathodes.

R_p (Ω cm^2)	R_o (Ω cm^2)	P (mW cm^{-2})	Cell components			Reference
			Cathode	Electrolyte	Anode	
0.09	0.16	620	PBC	20 μm SDC	Ni-SDC	[11]
0.09	0.14	810	SSC–SDC	10 μm SDC	Ni-SDC	[17]
0.60	0.15	578	LSCF–GDC	10 μm GDC	Ni-GDC	[30]
0.08	0.17	875	SDC–PBC	25 μm SDC	Ni-SDC	[29]
0.06	0.19	600	Impregnated PBC	26 μm SDC	Ni-SDC	This work

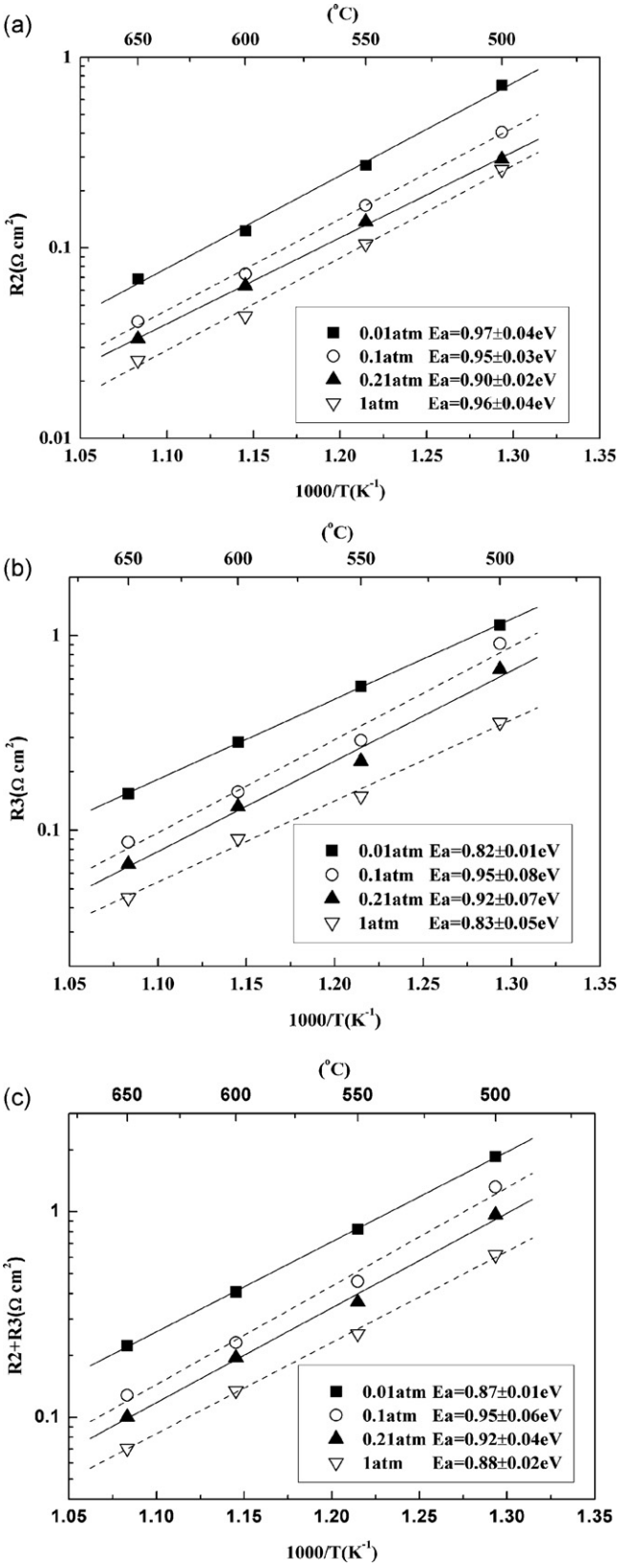

Fig. 7. Arrhenius plots of (a) R_2, (b) R_3, and (c) R_2+R_3 at various oxygen partial pressures.

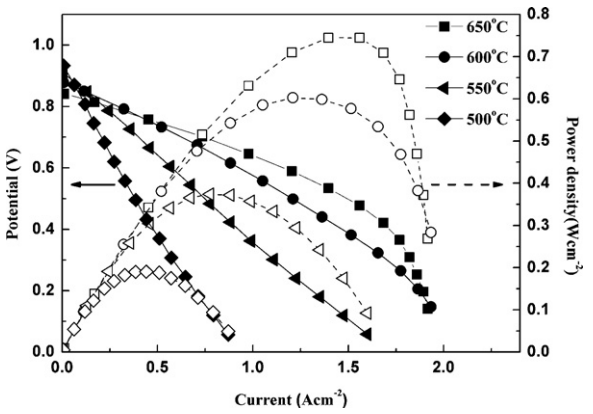

Fig. 8. PVI performance for anode-supported single cells with impregnated PBC cathodes.

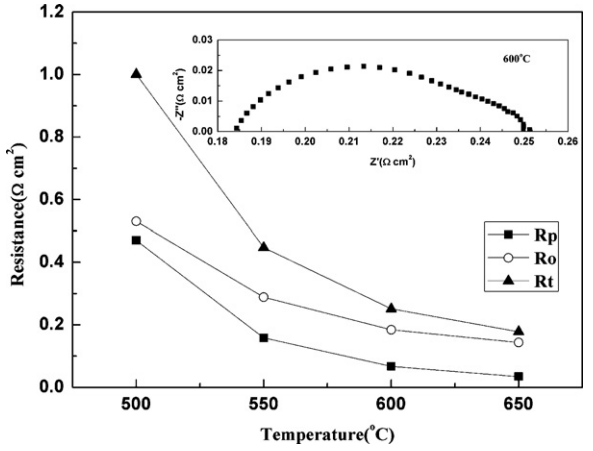

Fig. 9. The total cell resistance (R_t), interfacial polarization resistance (R_p) and ohmic resistance (R_o) as determined from the impedance spectra for anode-supported single cells with impregnated PBC cathodes measured from 500 to 650 °C under the open-circuit condition.

about 0.25 Ω cm^2, with 75% of which coming from the ohmic resistance, suggesting that the cell performance can be further improved by reducing the thickness of the electrolyte. The total electrode polarization resistance is only 0.06 Ω cm^2, much lower compared with those reported for impregnated SSC [17], LSCF [30], pure PBC [11], and SDC–PBC (30 wt.%) composite electrode [29] (as shown in Table 2). Further, it is smaller than 0.08 Ω cm^2 as measured with symmetrical cells for the cathode, possibly due to the activation effect on the impregnated cathodes when the inner current is passing though the cell because of the mixed conducting characteristics of the SDC electrolytes [31].

4. Conclusion

Layer-structure PBC nano-particles are formed with the ion impregnation method when it is fired at 800 °C. The crystalline size is about 20 nm while the particle size is 50 nm. With optimized loading, the PBC impregnated electrode has demonstrated interfacial polarization resistance as low as 0.082 Ω cm^2 at 600 °C, much lower than those of pure PBC electrode (0.86 Ω cm^2), PBC–SDC (30 wt.%) composite cathode (0.25 Ω cm^2) or various other impregnated cobaltite cathodes such as SSC (0.25 Ω cm^2), LSC (0.31 Ω cm^2), and LSCF (0.24 Ω cm^2). The dependence of the cathode impendence on oxygen partial pressure and the activation energy for the cathode interfacial resistance have revealed that the oxygen reduction process on the impregnated cathode is

mainly limited by oxygen ion incorporation at high frequency, electron charge transfer at middle frequency and gas diffusion steps at low frequency. The electrode reaction mechanism is very similar to that of pure PBC electrode, suggesting that impregnation does not change the electrode reaction process. However, both the oxygen ion incorporation and charge transfer steps are greatly accelerated due to the nanostructure of PBC fabricated by ion impregnation. Anode-supported single cells with the impregnated PBC cathode have achieved a maximum peak power density of 600 mW cm^{-2} at 600 °C, suggesting that impregnated PBC cathode is very promising cathode for intermediate temperature SOFC.

Acknowledgements

We gratefully acknowledge the financial support of the Ministry of Science and Technology of China (2012CB215403) and the US National Science Foundation (CBET 0967166).

References

[1] S.P. Jiang, J. Power Sources 124 (2003) 390–402.
[2] J. Hayd, L. Dieterle, U. Guntow, D. Gerthsen, E. Ivers-Tiffée, J. Power Sources 196 (2011) 7263–7270.
[3] M. Shah, S.A. Barnett, Solid State Ion. 179 (2008) 2059–2064.
[4] Z.P. Shao, S.M. Haile, Nature 431 (2004) 170–173.
[5] A. Maignan, C. Martin, D. Pelloquin, N. Nguyen, B. Raveau, J. Solid State Chem. 142 (1999) 247–260.
[6] G. Kim, S. Wang, A.J. Jacobson, L. Reimus, P. Brodersen, C.A. Mims, J. Mater. Chem. 17 (2007) 2500–2505.
[7] L. Wang, R. Merkle, J. Maier, T. Acartürk, U. Starke, Appl. Phys. Lett. 94 (2009) 071908.
[8] R.A. De Souza, J.A. Kilner, Solid State Ion. 106 (1998) 175–187.
[9] J.A. Lane, S.J. Benson, D. Waller, J.A. Kilner, Solid State Ion. 121 (1999) 201–208.
[10] A. Chang, S.J. Skinner, J.A. Kilner, Solid State Ion. 177 (2006) 2009–2011.
[11] D.J. Chen, R. Ran, K. Zhang, J. Wang, Z.P. Shao, J. Power Sources 188 (2009) 96–105.
[12] A. Tarancón, J. Peña-Martínez, D. Marrero-López, A. Morata, J.C. Ruiz-Morales, P. Núñez, Solid State Ion. 179 (2008) 2372–2378.
[13] T.Z. Sholklapper, H. Kurokawa, C.P. Jacobson, S.J. Visco, L.C. De Jonghe, Nano Lett. 7 (2007) 2136–2141.
[14] Z.Y. Jiang, C.R. Xia, F.L. Chen, Electrochim. Acta 55 (2010) 3595–3605.
[15] S.P. Jiang, W.Wang, J. Electrochem. Soc. 152 (2005) 1398–1408.
[16] J. Chen, F.L. Liang, L.N. Liu, S.P. Jiang, B. Chi, J. Pu, J. Li, J. Power Sources 183 (2008) 586–589.
[17] F. Zhao, R.R. Peng, C.R. Xia, Mater. Res. Bull. 43 (2008) 370–376.
[18] F. Zhao, L. Zhang, Z.Y. Jiang, C.R. Xia, F.L. Chen, J. Alloys Compd. 487 (2009) 781–785.
[19] Z.Y. Jiang, Z.W. Lei, B. Ding, C.R. Xia, F. Zhao, F.L. Chen, Int. J. Hydrogen Energy 35 (2010) 8322–8330.
[20] T.Z. Sholklapper, C. Lu, C.P. Jacobson, S.J. Visco, L.C.D. Jonghe, Electrochem. Solid State Lett. 9 (2006) 376–378.
[21] Y. Huang, K. Ahn, J.M. Vohs, R.J. Gorte, J. Electrochem. Soc. 151 (2004) 1592–1597.
[22] W. Zhu, D. Ding, C.R. Xia, Electrochem. Solid State Lett. 11 (2008) 83–86.
[23] H. Zhang, F. Zhao, F.L. Chen, C.R. Xia, Solid State Ion. 192 (2011) 591–594.
[24] X.Y. Xu, C.B. Cao, C.R. Xia, D.K. Peng, Ceram. Int. 35 (2009) 2213–2218.
[25] J.-D. Kim, G.-D. Kim, J.-W. Moon, Y.-I. Park, W.-H. Lee, K. Kobayashi, M. Nagai, C.-E. Kim, Solid State Ion. 143 (2001) 379–389.
[26] X.J. Chen, K.A. Khor, S.H. Chan, J. Power Sources 123 (2003) 17–25.
[27] Y. Takeda, R. Kanno, M. Noda, Y. Tomida, O. Yamamoto, J. Electrochem. Soc. 134 (1987) 2656–2661.
[28] N.T. Hart, N.P. Brandon, M.J. Day, J.E. Shemilt, J. Mater. Sci. 36 (2001) 1077–1085.
[29] D.J. Chen, R. Ran, Z.P. Shao, J. Power Sources 195 (2010) 7187–7195.
[30] Y.J. Leng, S.H. Chan, S.P. Jiang, Solid State Ion. 170 (2004) 9–15.
[31] M. Mogensen, N.M. Sammes, G.A. Tompsett, Solid State Ion. 129 (2000) 63–94.